JOURNAL OF GEOPHYSICAL RESEARCH, VOL. 96, NO. D12, PAGES 22,673–22,682, DECEMBER 20, 1991

The Inflatable Sphere: A Technique for the Accurate Measurement of Middle Atmosphere Temperatures

F. J. SCHMIDLIN

NASA GSFC/Wallops Flight Facility, Wallops Island, Virginia

H. S. LEE

Science and Engineering Services, Incorporated, Silver Spring, Maryland

W. MICHEL

University of Dayton Research Institute, Wallops Island, Virginia

In recent years there has been increasing interest in the utilization of the inflatable falling sphere technique for middle atmosphere studies. The falling sphere technique uses radar position information and the equation of motion to calculate density data from which temperature information is derived. Through theoretical derivation, simulation, and measurements it is demonstrated that the temperatures derived from falling spheres are not significantly affected by linear bias in the density measurements that originate from uncertainties in sphere mass, volume, or cross-sectional area. This study illustrates the sphere's capability to produce accurate temperatures up to 85 km and higher, given that the necessary reduction initialization conditions are met. At heights below 60 km, comparison of sphere temperatures with in situ thermistor measurements obtained close in space and time shows good agreement. Comparison with OH-radical rotational temperatures also confirms excellent agreement at 86 km. It is concluded that the sphere technique is an independent and highly accurate source of temperature measurement, is unique in being the only low-cost source of in situ measurement of temperature throughout the mesosphere and lower thermosphere, and qualifies as an intrinsic method to establish the accuracy of other atmospheric measurement systems.

1. INTRODUCTION

During the past two decades there has been considerable interest expressed in middle atmosphere temperature measurements, their influence on the motions and dynamics of the region, their interrelationship with chemical species and the electrical structure, and in general the morphology of events occurring there. Numerous studies of temperature trends, turbulence in the mesosphere and higher, electrodynamic interaction between the ionosphere and neutral atmosphere, gravity and planetary wave influence on energy exchange, etc., have been conducted. There also exists a need for precise ground truth measurements to verify retrieved temperatures from existing remote sensors and from the future generation of satellite instruments planned to fly on UARS, EOS, and others. These studies and ground truth requirements have exacerbated the need for accurate in situ temperature measurements to altitudes higher than previously available.

Satellite instruments ideally provide continual monitoring of temperature, but there are often discontinuities in the retrievals when one satellite replaces another. Ground-based techniques, such as lidar, are relatively new and still undergoing development and testing. Thus the temperature measurements provided by the low-cost, small meteorological rocketsonde stand alone as the long-term (i.e., >20 years) upper stratosphere and lower mesosphere data source. Another advantage of rocket measurements is the detailed vertical profiles that are provided and used in the many different types of atmospheric studies. In spite of the rocketsonde's long-term record and high resolution, questions are often asked about its measurement accuracy and precision.

In the past, measurements up to 90 km and higher were obtained with very expensive and sophisticated instrumentation such as pitot probes, acoustic grenades, and the active falling sphere. The pitot probe measures densities from which temperatures are derived. This technique provides density and temperature data to an accuracy of about 5% to 120 km altitude and about 2% between 60 and 90 km [*Horvath and Theon*, 1972]. Temperatures and densities from a small meteorological rocketsonde provided "ground" truth at the lower end of the pitot probe's measurement. Because of the cost and complexity of the pitot probe there generally were only a few launchings per year, and it has not been used since the early to mid-1970s. Similarly, the acoustic grenade technique provided a measurement of the speed of sound between 30 and 90 km, from which temperatures and winds were derived [*Smith et al.*, 1968; *Theon et al.*, 1972]. This also was an expensive measurement and required an extensive array of supersensitive microphones as well as a complex data reduction procedure. Because of the high sensitivity of the microphones, unacceptable noise interference occasionally inhibited the launching of the grenade system. Thus measurements keyed to definitive times for unique purposes were often difficult to obtain. Temperature measurement accuracy was of the order of 3°–5°K and

Paper number 91JD02395.
0148-0227/91/91JD-02395$05.00

depended on the microphone locations, length of baseline, etc. Finally, the active falling sphere used accelerometers and sophisticated telemetry making complex reduction procedures necessary [*Philbrick et al.*, 1985]. The active falling sphere provided temperature data between 50 and 150 km. Because of the cost of the hardware, launching, and acquisition of the data its use has been discontinued.

The above discussed techniques are not cost effective or practicable for frequent use, and yet there is still a very strong requirement for accurate temperature data above 60 km. To meet this requirement, a very strong dependence on data obtained from the inflatable falling sphere has developed within the science community. We will show in this paper that the passive falling sphere method, although not measuring temperature directly, is a viable and accurate source of temperature data.

2. BACKGROUND

Two rocketsonde instruments widely used since about 1969 to gather middle atmosphere temperature, density, pressure, and wind data are the Super Loki Datasonde and Super Loki sphere. Until recently, about 2000 launchings a year took place at 20–25 launch sites. This number has now decreased to a few hundred launchings per year and the number of launch sites operated by the United States has decreased to eight. Fewer launchings and the exodus of the large sophisticated rocket systems make it necessary that the measurements that are available be reliable and well utilized. Thus the accuracy and precision of the measurement techniques are important.

Accuracy of high altitude in situ temperature-measuring instruments is difficult to obtain since the measurement dynamics are not simple and a standard reference instrument is not available for comparisons. Comparisons between in situ high altitude instruments [*Finger et al.*, 1975] or with in situ and remote techniques, such as lidars or satellites, generally agree within a temperature envelope of 10°K [*Schmidlin*, 1984]. This agreement has been considered as an estimate of instrument accuracy [*Schmidlin*, 1986], but it is necessary to recognize that accurate and more precise instruments are needed to satisfy the requirements of atmospheric investigations, for example, the analysis to detect global temperature trends [*Angell*, 1987].

The need to better define the temperature measurement accuracy of the in situ instrumentation led to definitive studies at NASA's Wallops Flight Facility. These efforts follow earlier simulation studies of the inflatable falling sphere carried out to improve the filtering methods used in data reduction. These simulations pointed out that the falling sphere might be an intrinsic method that could be used to establish the measurement accuracy of other in situ systems as well as remote systems.

The inflatable sphere method was developed about 30 years ago to obtain atmospheric soundings between 30 and 60 km [*Leviton and Palmquist*, 1960]. Requirements to extend the measurements above 60 km led to improvements in the reduction software [*Luers*, 1970; *Engler*, 1965]. The inflatable sphere is a simple 1-m-diameter mylar balloon containing an inflation mechanism and nominally weighs about 155 g. The sphere normally is deployed at an altitude of approximately 115 km where it free-falls under gravitational and wind forces. The sphere, after being deployed, is inflated to a superpressure of approximately 10–12 hPa by the vaporization of a liquid, such as isopentane. The surface of the sphere is metalized to enable radar tracking for position information as a function of time. To achieve the accuracy and precision desired, the radar must be a high precision tracking system such as an FPS-16 C-band radar or better. The radar-measured position information and the coefficient of drag are then used in the equations of motion to calculate atmospheric density and winds. The calculation of density requires knowledge of the sphere's coefficient of drag over a wide range of flow conditions [*Luers*, 1970; *Engler and Luers*, 1978]. Pressure and temperature are also calculated for the same altitude increments as the density.

Sphere measurements are only affected by the external physical forces of gravity, drag acceleration, and winds which make them a potentially more accurate measurement than other in situ measurements. *Engler and Dietenberger* [1978] discuss a comparison of inflatable sphere temperature measurements with those from in situ bead thermistor measurements and give a summary of the measurement error of the sphere technique due to the effect of vertical winds. The vertical winds associated with gravity waves are random in nature, and they appear as random perturbations in the density calculation. The mean vertical winds associated with the large-scale circulation are sufficiently small (several centimeters per second), compared with the sphere's fall velocity (several hundred meters per second), that they can be neglected. For the sphere measurement technique to work well, it must, of course, also be properly inflated and not leaking.

In contrast to the passive sphere measurements the Super Loki Datasonde temperature measurements are made by a small bead thermistor as the instrument descends on a parachute. The measurements made with the Datasonde are influenced by a number of external factors. For example, the main contribution to the measurement error comes from aerodynamic heating, long-wave and short-wave radiation, sensor lag, sensor emissivity, and measuring current heating. Although a system of corrections is employed [*Krumins and Lyons*, 1972], it provides only nominal corrections, and in some situations, large residual errors may remain, which are not explained by the correction technique. The Datasonde measurements begin immediately after the deployment of the payload, usually near 80 km. The wind data become acceptable near 72 km, after the decelerator has fully inflated and begins to measure the horizontal wind. Temperature measurements begin at 70 km, although there is some doubt at what altitude they become valid [*Schmidlin*, 1981]. Because of these limitations in altitude coverage and measurement accuracy a relatively inexpensive and accurate high altitude system, such as the falling sphere, is desirable.

3. MEASUREMENT THEORY

Early data reduction software design limited the inflatable sphere density measurement error to 2% or less over the altitude range of the observation [*Luers*, 1970]. The software effectively accomplishes this by use of polynomial fitting of each data segment. However, the length of the filters required to meet this condition is quite long and, above 60 km altitude, limits the vertical resolution to 5 km or more. While attempting to improve the measurement resolution through simulation studies [*Schmidlin et al.*, 1985, 1987], it was realized that the inflatable sphere technique can provide

accurate (unbiased) temperature measurements. In order to understand how the sphere technique provides accurate temperature measurements an understanding of its measurement physics is important.

The motion of the falling sphere is described by a simple equation of motion in a frame of reference having its origin at the center of the Earth, as

$$m\frac{d\vec{v}}{dt} = -m\vec{g} - \frac{\rho C_d A_s v_r^2 \hat{v}_r}{2} - \rho V_b \vec{g} - 2m\vec{\omega} \times \vec{v}, \quad (1)$$

where m is the sphere's mass, $\vec{g}$ the acceleration due to gravity, $\vec{\omega}$ the Earth's angular velocity, $\vec{v}$ the sphere's velocity, ρ the atmospheric density, and V_b the volume of the sphere. The relative velocity of the sphere with respect to the air mass is defined as $\vec{v}_r = \vec{v} - \vec{w}$, where $\vec{w}$ is the wind velocity. In (1), $\hat{v}_r$ denotes the unit vector. Therefore the drag coefficient C_d is calculated on the basis of the relative velocity of the sphere. The terms on the right side of (1) represent the gravity, friction, buoyancy, and coriolis forces, respectively. Note that the wind effect enters only in the friction force term in terms of relative velocity of the sphere with respect to the air mass moving with the wind velocity.

After simple mathematical manipulation, (1) is decomposed into three orthogonal components, including the vertical component of the equation of motion from which the density is calculated; thus

$$\rho = \frac{2m(\ddot{z} - g_z - C_z)}{C_d A_s |v_r|(\dot{z} - w_z) + 2V_b g_z}, \quad (2)$$

where $\ddot{z}$ is the vertical component of the sphere's acceleration, $\dot{z}$ is the vertical component of its velocity, A_s is the sphere's cross-sectional area, and v_r is the motion of the sphere relative to the air. The magnitudes of the buoyancy force ($V_b g_z$) and the coriolis force (C_z) terms compared to the other terms of (2) are small and are treated as perturbations.

The temperature profile is extracted from the retrieved atmospheric density (equation (2)) using the hydrostatic equation and the equation of state as follows:

$$T_z = T_a \frac{\rho_a}{\rho_z} + \frac{M_0}{R\rho_z}\int_z^a \rho_{z'} g\, dz', \quad (3)$$

where ρ_z is the density at altitude z, ρ_a is the density at a reference altitude a, M_0 is the molecular weight of dry air, R is the universal gas constant, and T is the temperature in degrees Kelvin. Note that the source of temperature error is the uncertainty associated with the retrieved density value. This density error is comprised of high and low spatial frequency components. The high frequency component may arise from many sources, such as measurement error, computational error, and/or atmospheric variability and is somewhat random. Nonetheless, the error amplitude may be suppressed by statistical averaging. On the other hand, the low frequency component, including a bias and linear variation, may be related to actual atmospheric features and is indistinguishable from the measurement error. In spite of density errors that may arise from the uncertainties of the various measurement parameters, the temperature calculation is virtually unaffected by the bias and linear components of the density error, as will be shown below.

The use of an assumed standard atmospheric pressure and temperature in (3) for the initial points in the processing of sphere trajectory data leads to an uncertainty in the retrieved temperature values for approximately two scale heights below the initial point of reduction. As pointed out by *Quiroz and Gelman* [1976], the reality of the temperatures above 90 km would be difficult to establish considering the influence from the first-guess temperature. However, assuming that the initial data reduction point occurs at approximately 98 km (typical for a properly performing sphere trajectory), the temperature error at an altitude of two scale heights lower is considerably reduced, and the accuracy of the sphere temperature below this altitude becomes very high. Parameterization by way of independent tests using two standard atmosphere models to supply the initialization data differing by 20°K at 98 km resulted in temperature agreement between the two reductions of 4°K at 85 km. Thus the reliability of the retrieved temperatures over the altitude region of the scale-height effect is highly dependent on how close the initial guess temperature is to the real temperature. *Luers* [1970] pointed out that a 10% error in the initial temperature diminishes to 1% or less after 10 km and that the temperature error due to noise in the reduction of density is less than 2% below 90 km altitude. Note that the magnitude of the first term in (3) compared to the second term becomes negligible as the sphere descends in altitude. Thus for this region we can approximate (3) as

$$T_z = \frac{M_0}{R\rho_z}\int_z^a \rho(z') g\, dz'. \quad (4)$$

To study the density bias effect on the temperature retrieval, the bias is modeled as

$$\rho(z) = \rho_t(z)(1 + A + Bz + Cz^2 + \cdots), \quad (5)$$

where $\rho_t(z)$ is the true density and A, B, and C are constants. Uncertainties in system parameters of the experiment, such as sphere size, mass, and coefficient of drag, may be the sources of the constant bias represented by the second term in (5). The remaining low frequency contribution to the bias may originate from a slowly leaking sphere, sphere deformation, functional behavior of the uncertainty in drag coefficient, or other, more complex sources. Only the first three terms in (5) are considered for simplicity.

From (4) and (5) we derive

$$T_z = \frac{M_0}{R\rho_z}\int_z^a \rho_t(z') g[(1 + A) + Bz']\, dz'. \quad (6)$$

Using an ideal exponential atmospheric density profile represented by

$$\rho_t(z) = \rho_0 e^{-z/\sigma} \quad (7)$$

where σ is a constant density scale height, for the $\rho_t(z')$ in the integrand, we integrate (6)

$$T_z = \frac{M_0}{R\rho_t(z)} g\sigma\rho_0 e^{-z/\sigma} \quad (8)$$

after a few steps of simplification. Note that the terms involving $e^{-a/\sigma}$ tend to zero due to the large initial altitude

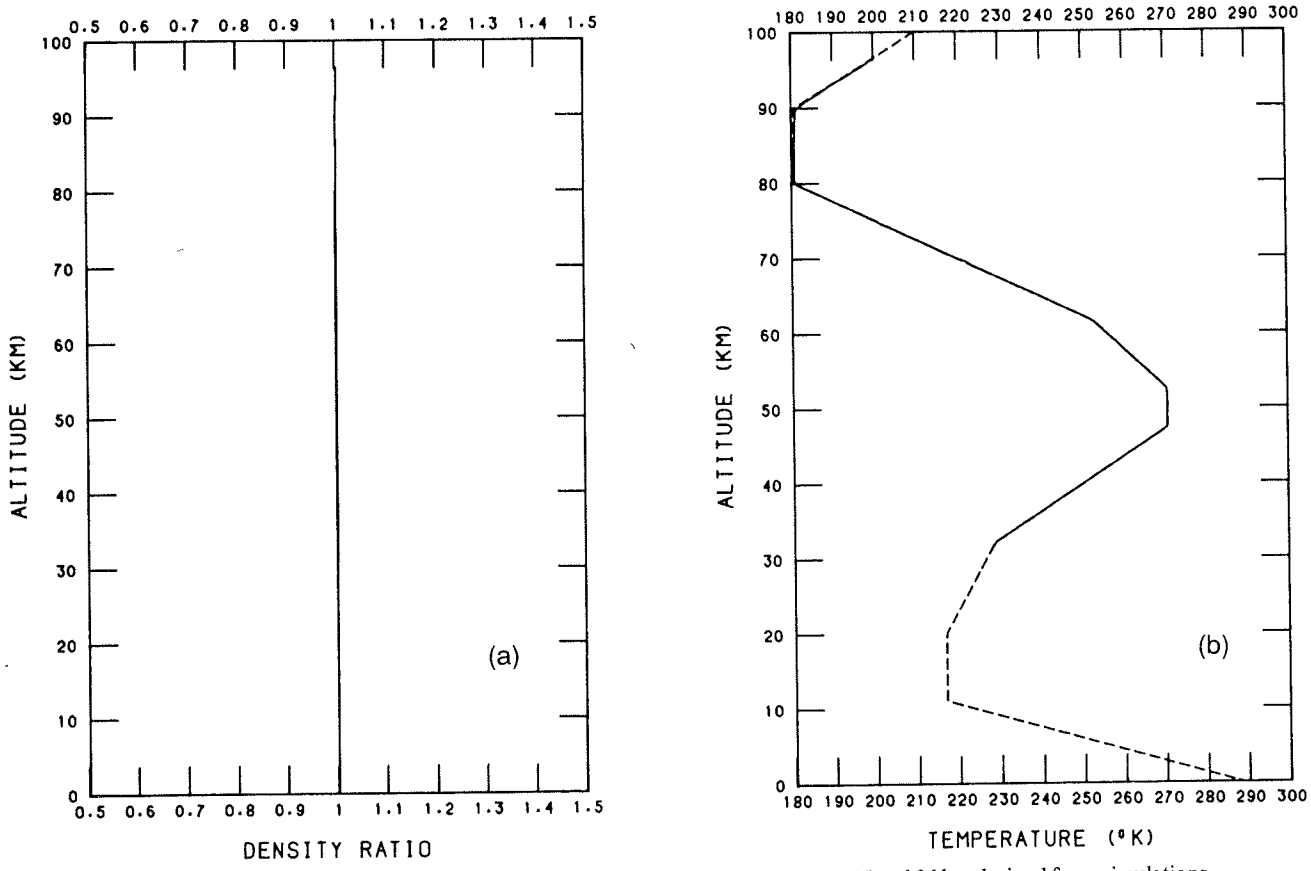

Fig. 1. (*a*) Ratio of retrieved versus *COESA* [1976] densities (ρ_z/ρ_{76}) between 35 and 96 km derived from simulations. (*b*) Comparison between simulated falling sphere temperatures and the *COESA* [1976] temperatures.

value. The actual atmospheric density scale height is a weak function of altitude up to approximately 100 km; thus the use of an exponential atmosphere is a reasonable approach. The actual altitude-dependent scale height effect cannot be readily handled in closed form. Therefore we perform an extensive simulation study to examine the effect of a more realistic atmosphere where the altitude-dependent scale height is fully accounted for through a model temperature profile.

The temperature retrieved from the sphere density is free from the input bias term represented in (5) and depends only on the true density, as (8) clearly indicates. The effect of higher order terms in (5) will not be removed in the temperature retrieval. However, examination of sphere profiles suggests that the occurrence of such a high order bias is not frequent.

4. Flight Simulations

The unique characteristics of the temperature retrieval was subjected to tests using computer simulation methods designed to study the inflatable sphere technique. Densities from the *Committee for the Extension of the U.S. Standard Atmosphere* (*COESA*) [1976] were used as the baseline atmosphere. The simulations were carried out by releasing standard weight spheres (~155 g) from an assumed altitude of 120 k. The equation of motion for a falling sphere was solved. Radar angles and slant ranges were successively derived at time increments of 0.1 s corresponding to the falling sphere's sequential positions. The simulated radar information did not contain angular and slant range tracking errors nor noise which is present in actual radar tracking data, so that the interpretation would not be distorted. These radar data were then submitted to the standard operational software for reduction. The derived densities were found to be equivalent to the *COESA* [1976] densities used in the simulation. More importantly, the corresponding *COESA* [1976] temperatures were retrieved in the reduction, although temperature information was not a direct input to the simulation program.

Figure 1*a* shows an example of the agreement between the simulated and derived densities. Since there are 4 orders of magnitude change in density between 30 and 90 km, the observed density is presented as a ratio to the *COESA* [1976] density (i.e., ρ_z/ρ_{76}). A ratio of 1 indicates that the retrieved densities are equivalent to the standard atmosphere densities at the same altitudes. Figure 1*b* shows the temperatures derived following (8) together with the *COESA* [1976] temperatures. The agreement is almost perfect.

Consideration was given to how well the reduction technique could handle biased data. For example, if the sphere mass or diameter is in error by some small percentage, it is known that the retrieved density will be in error by a proportional amount [*Luers*, 1970]. That is, a 5% error in sphere mass will result in a 5% error in calculated atmospheric density. However, given that such an error in density occurs, should it be expected that the retrieved temperatures will have corresponding errors? Figure 2*a* is an example of the retrieved density versus the *COESA* [1976]

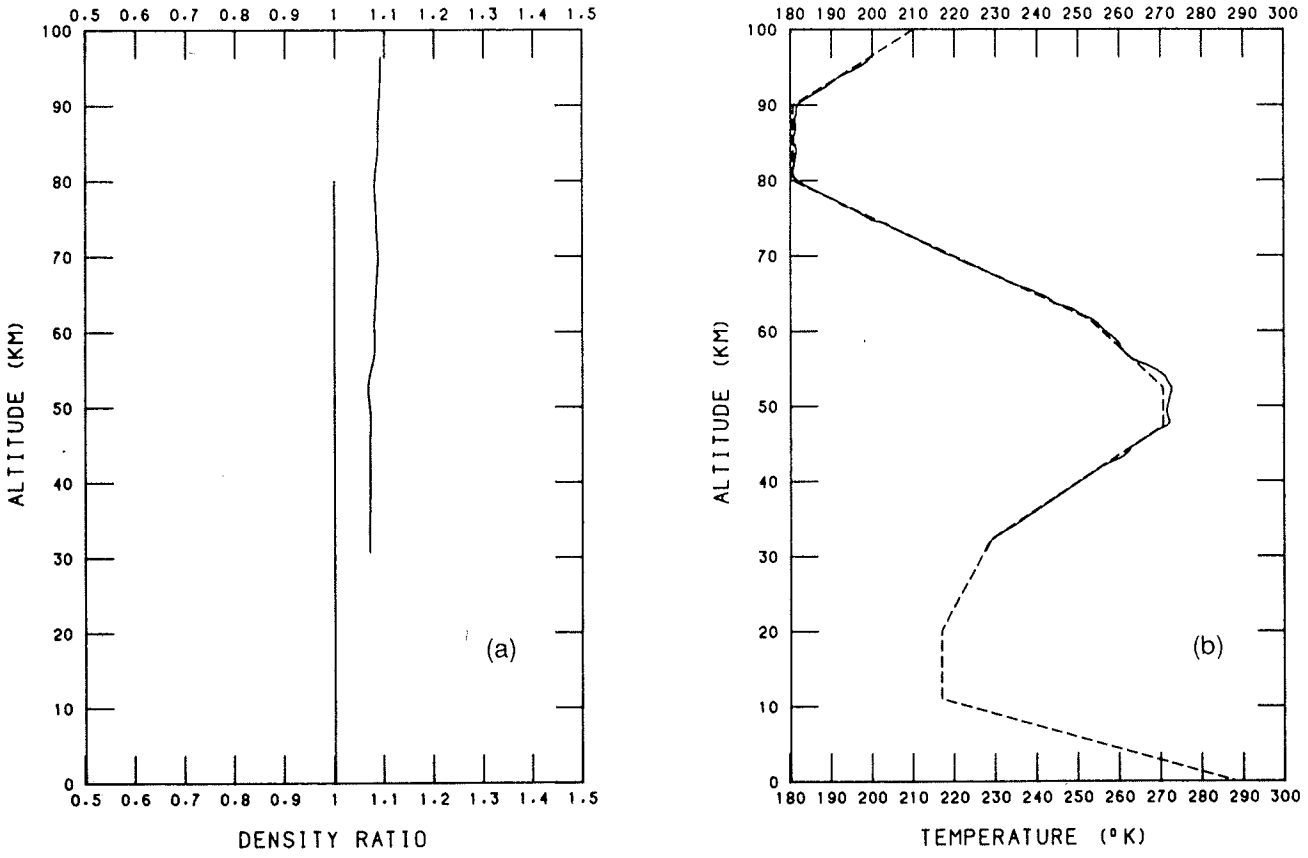

Fig. 2. (*a*) Ratio of retrieved versus *COESA* [1976] densities (ρ_z/ρ_{76}) after changing sphere weight by 7%. (*b*) Example of the agreement between temperatures reduced from a linear density bias and the *COESA* [1976] temperatures. The differences observed near 50 km are about 1%.

density with a 7% reduction in the sphere weight in the simulation. A lighter sphere will fall slower resulting in a higher calculated density. Clearly, the recovered density has a corresponding bias proportional to the error in the sphere's weight. More importantly, however, the corresponding retrieved temperatures are in good agreement with the *COESA* [1976] temperatures, as shown in Figure 2*b*. The exception is the region near 50 km where a difference from the expected temperature is about 3°K or 1%. Furthermore, a range of biases was tested in the simulations and showed that the bias can be substantially large (e.g., greater than 20%) before a significant temperature error occurs.

On the other hand, a slowly leaking sphere, as might occur if there is a "pin hole" in the mylar skin, causes an increasing density bias versus altitude, as shown in Figure 3*a*. However, a slowly leaking sphere will still permit a temperature retrieval with an error of 5% or less, as illustrated in Figure 3*b*.

The implication of our simulation study and analysis is that the temperature retrievals from falling spheres are not significantly affected by errors in density caused by uncertainties in either sphere mass, volume, or cross-sectional area (i.e., the primary sources of errors due to linear effects, as shown in (5)). Furthermore, a small leak in the sphere may not be a serious problem in accepting the temperatures as usable, so long as the leak rate is small and the sphere maintains its volume (rigidity) within a certain fraction. However, there does not presently exist an objective test to determine whether or not a leak exists; this requires a subjective decision after inspection of the records. Thus it is clear that well functioning spheres will totally satisfy the accuracy results discussed here, while linear bias in density or a slowly leaking sphere will yield temperatures accurate to within 2%. Nevertheless, careful evaluation of the behavior of the sphere is essential before assuming the validity of the data.

5. Measurement Comparisons

Comparison of temperature measurements obtained with the inflatable sphere and Datasonde are discussed in the two examples below. These provide further evidence of the inflatable sphere's capability to produce accurate temperatures. To understand these examples, it should be borne in mind that radar noise and vertical winds are present in the data that give rise to the perturbations seen below 60 km altitude. Furthermore, the comparisons shown in these examples also demonstrate a probable deficiency in the reported measurements of the Datasonde at levels above 60 km.

Example 1, April 22, 1987

The first example compares density and temperature measurements from an inflatable sphere and Datasonde launched 21 min apart on April 22, 1987. Although these measurements were not made simultaneously, they should correlate well since atmospheric changes usually occur slowly during late spring. In the example given, sphere temperatures begin

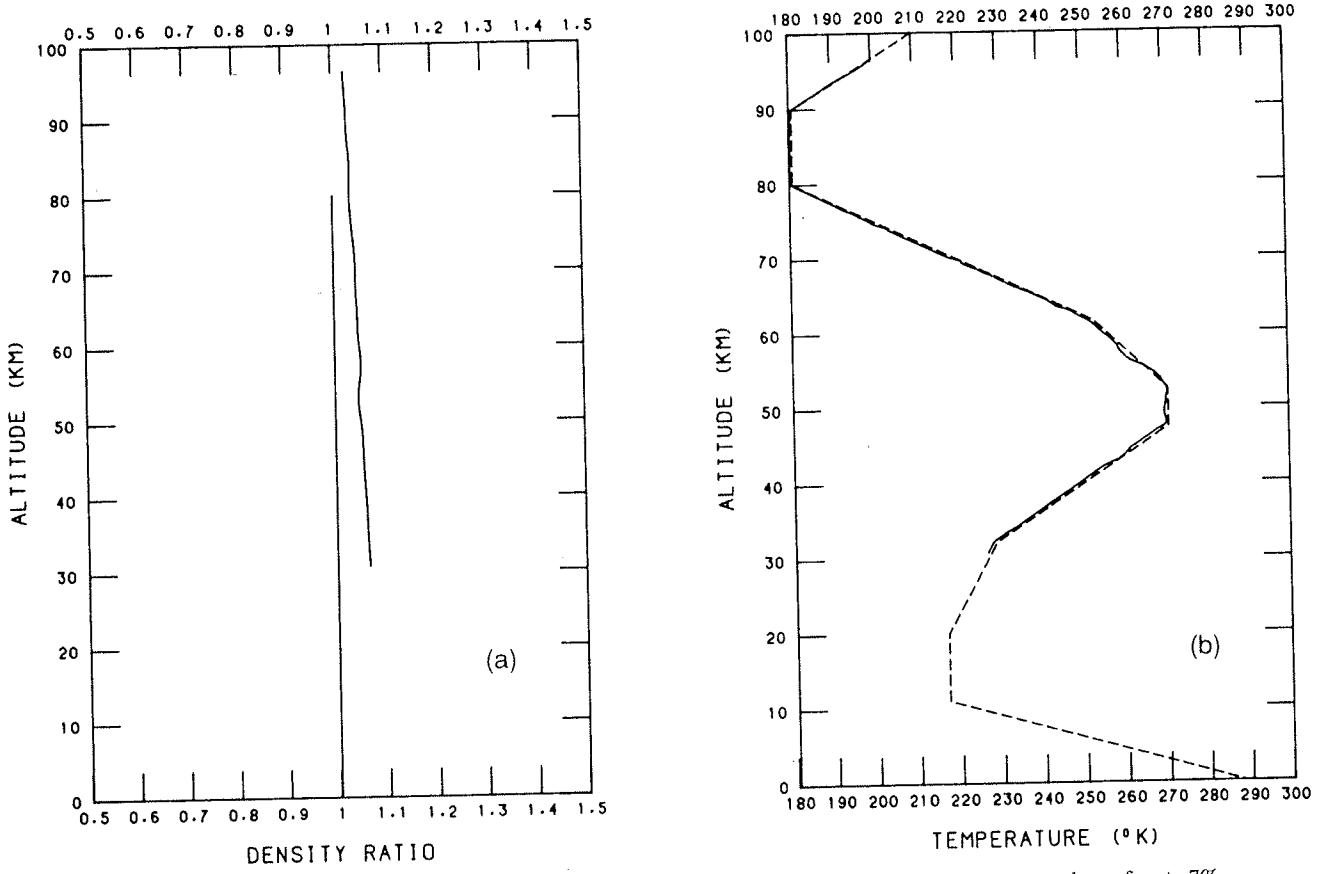

Fig. 3. (*a*) Ratio of retrieved versus *COESA* [1976] densities (ρ_z/ρ_{76}) after assuming a sphere mass loss of up to 7% due to a leaking sphere. (*b*) Resulting temperature agreement with *COESA* [1976] temperatures. Differences are less than 1%.

near 85 km with sphere collapse occurring near 35 km. The Datasonde temperatures, on the other hand, begin near 70 km and end at 20 km. The density measurements made by each system are shown in Figure 4*a*, where the ratios ρ_z/ρ_{76} for the sphere and Datasonde are plotted, respectively. A bias of about 6% exists below 60 km. However, the observed profiles are otherwise similar in many respects. Between 60 and 70 km there is no apparent bias. Below 60 km in spite of the bias and small differences observed, it is obvious that the sphere and Datasonde are tracing the same density structure.

Our postulation that the sphere temperature profiles would be accurate in spite of density bias is well justified, based on the relatively good agreement between the temperature profiles in Figure 4*b*. Comparison below 35 km was not possible in this example because of the collapsed sphere. Above 60 km, where we claim that the sphere data are valid, the Datasonde's temperatures are higher. Since the sphere temperatures agree with the Datasonde temperatures throughout the layer below 60 km, new densities were calculated using upward integration. This was accomplished by merging the sphere temperatures with the Datasonde temperatures near 35 km. (Although in this case the high altitude support radiosonde observation could have been used.) A comparison of the sphere's new densities with the Datasonde densities are shown in Figure 4*c*. Clearly, there is considerable improvement in agreement between the density profiles.

At 60 km and higher, however, the densities now disagree in contrast to the previous agreement noted in Figure 4*a*. Because of the excellent temperature agreement at altitudes below 60 km and the sphere data characteristics discussed in previous sections, we argue that the sphere temperatures are accurate regardless of bias error in the densities throughout the altitude range of 85 to 30 km. This argument suggests that the Datasonde's temperature measurements at altitudes above 60 km are in error. Indeed, this is the region where the Datasonde thermistor diameter is smaller than the atmosphere's molecular mean free path and where the temperature corrections were extrapolated upward from 60 km.

Vertical winds are believed to be, at least partially, the cause of the observed perturbations in the sphere data below 60 km. Vertical winds, depending upon whether downward or upward directed, will cause the sphere to accelerate or decelerate as it falls. These changes in acceleration then appear as changes or perturbations in density. If it were possible to measure the vertical wind and remove it before performing the density reduction, the remaining perturbations would be those actually occurring in the density field. Density perturbations translate into perturbations in pressure and temperature. Note that the effect of the perturbation does not persist as the sphere descends since the effect of the perturbation on pressure decays fast, and the density is derived from the local variables. It is these perturbations that most likely account for the small differences noted between the profiles (time differences between the sphere and Datasonde observations, although relatively short, may also be a contributing factor). The perturbation temperature differences are generally less than 5°C.

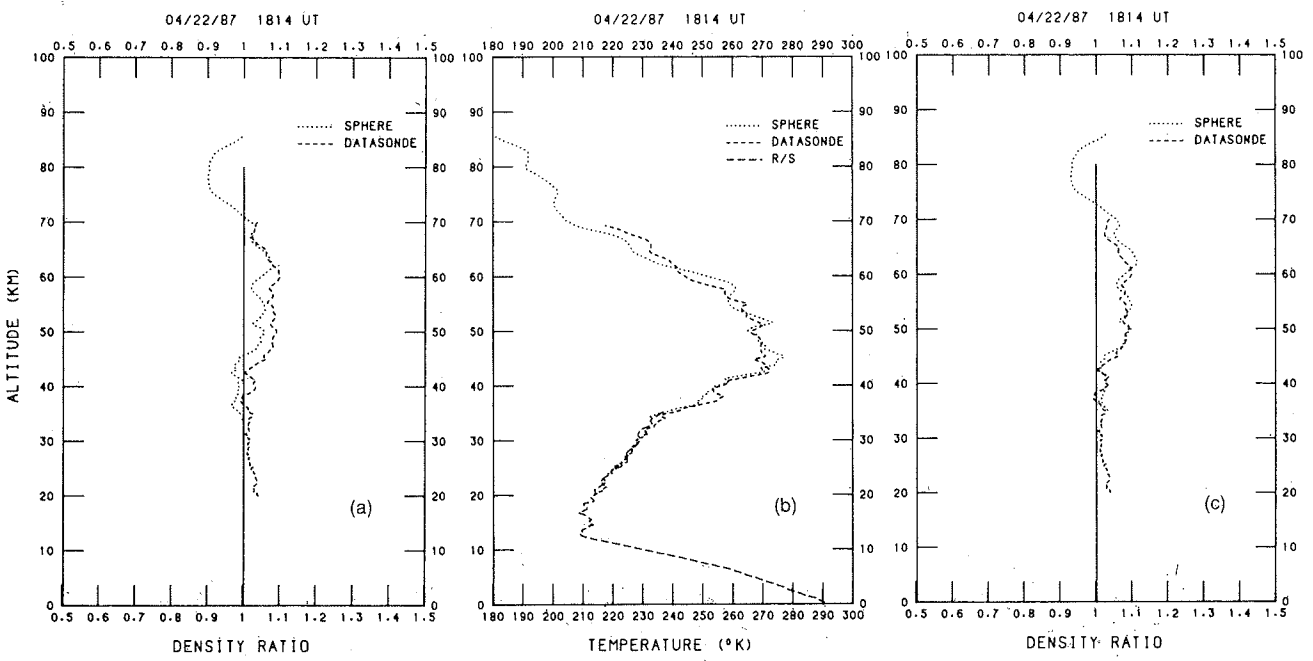

Fig. 4. (*a*) Comparison of density ratios (ρ_z/ρ_{76}) between sphere and Datasonde measurements. An approximate 6% bias is present below 60 km. (*b*) Comparison of temperatures between sphere and Datasonde in situ measurements showing agreement between 60 and 35 km where the sphere begins to collapse. (*c*) Sphere densities recalculated from an initial level of integration near 35 km and compared with Datasonde-measured densities.

Example 2, April 23, 1988

The second example presents additional evidence that temperatures derived from sphere-measured densities are generally accurate. The sphere and Datasonde density profiles, shown in Figure 5*a*, are in good agreement below 60 km. As shown in Figure 5*b*, the corresponding temperature profiles below 60 km are also in relatively good agreement. Although the sphere data acquired on April 23 show a larger number of perturbations than were seen on April 22, many of the perturbations correlate well with the perturbations of the Datasonde. Those perturbations not in agreement indicate about a 2% difference, or less than 5°C. Furthermore, at altitudes near 30 km there is excellent agreement among the Datasonde, sphere, and radiosonde temperatures. This is important because it suggests that consistent temperature measurements are present from the three techniques. Nev-

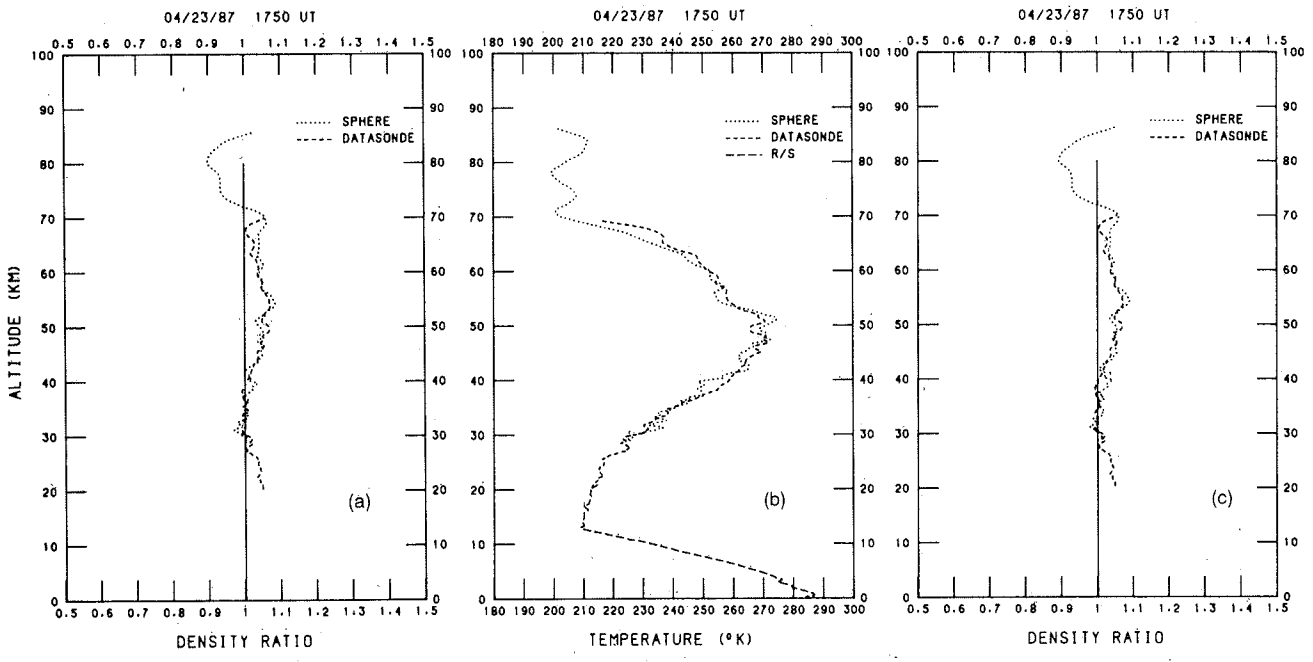

Fig. 5. (*a*) Same as Figure 4*a*, except that no bias exists between sphere and Datasonde densities. (*b*) Same as Figure 4*b*, except sphere collapsed near 30 km. (*c*) Same as Figure 4*c*.

ertheless, at altitudes between 60 and 70 km a bias is observed between the temperature profiles of the two rocketsonde techniques. Note the disagreement in the density profiles above 60 km in Figure 5*a*.

Using the Datasonde's density and the sphere's temperature to initialize the integration, densities corresponding to the sphere temperatures and heights were recalculated by integrating the hypsometric equation upward. As Figure 5*c* indicates, little change is noted from the originally derived densities shown in Figure 5*a*. This suggests that the sphere data probably were initially correct. The disagreement in temperatures above 60 km as seen in Figures 4*b* and 5*b*, however, consistently appears in sphere/Datasonde comparisons. Density agreement or disagreement, as seen in Figures 4*a* and 5*a*, reflect the presence of bias in the sphere density reduction. Clearly, in both examples discussed, it appears that the Datasonde temperatures are too high at altitudes above 60 km. This does not answer the question of why a density bias exists in the measurement on April 22 but does support our claim concerning temperature accuracy of the falling sphere. Given accurate temperatures, the correct density will be retrieved by upward integration. In most cases, data from a high altitude radiosonde observation could supply the needed initial tie-on point for this integration.

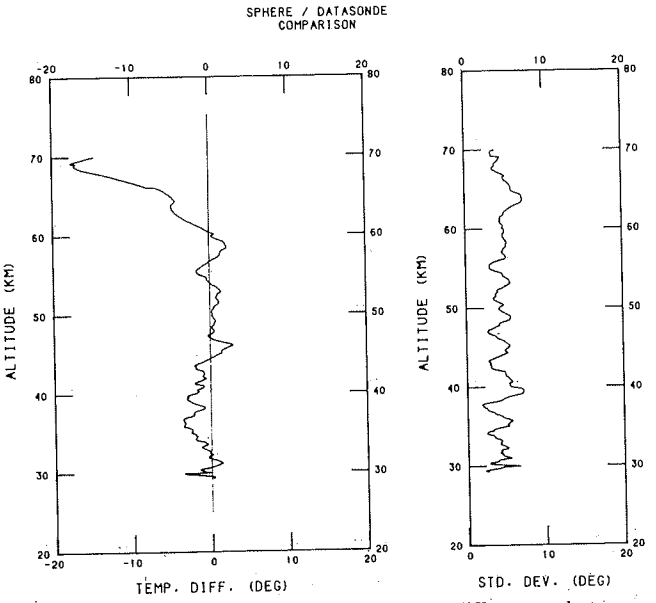

Fig. 6. Comparison of mean temperature differences between sphere and datasonde measurements showing poor agreement above 60 km altitude. The mean differences (~3°K) below 60 km are less than the standard deviations of the paired differences (~5°K).

6. OTHER COMPARISONS

Extending our discussion of sphere temperature measurement accuracy, it is desirable to mention other correlative measurements that included spheres and Datasondes. Earlier measurements of sphere temperatures in the mesosphere showed good agreement with the acoustic grenade technique [*Olsen and Schmidlin*, 1978]. Comparisons between inflatable spheres and accelerometer spheres [*Philbrick et al.*, 1978, 1985] also indicated agreement within 5%. Considering the difficulty of making accurate temperature measurements at 60 km and higher, investigators of atmospheric dynamics of the mesosphere readily accept an error of 5–10%. However, a recent study carried out in northern Norway demonstrated the comparability of sphere temperature measurements near 90 km with an ionization gage, a mass spectrometer, and lidar. *Lübkin and von Zahn* [1989] pointed out differences in temperature measurements between these instruments of less than 10°K.

An example of mean differences between sphere temperatures and Datasonde in situ temperatures is illustrated in Figure 6, where differences generally less than 3°C are shown. Although there are numerous pairs of profiles from many different sites available for comparison, 14 pairs were selected from Wallops Island and from Andenes, Norway. Figure 6 illustrates two features worthy of discussion in addition to the relatively small mean differences. The first feature is the difference between sphere and datasonde temperatures at altitudes above 60 km. From Figure 6 it is clear that the Datasonde temperatures are higher than those reported by sphere measurements. Near 60 km the difference is small, approximately 0°C; however, at 70 km the datasonde mean temperature is higher than the sphere mean temperature by 15°K.

The second feature is the "S"-shaped bias between 30 and 60 km. Between 48 and 60 km the bias reaches a maximum value of about 2°C. In this layer the Datasonde temperatures are lower than the sphere temperatures. Between 30 and 48 km the Datasonde mean temperature is higher than the sphere mean temperature, approaching a 3°C difference. The amplitude of this feature is well within the standard deviation of the differences between the pairs. However, it is a significant bias feature because of its long wavelength and is not just random noise. There is a possibility that the reason for the S-shaped bias may simply be due to time lag of the Datasonde thermistor response. While the overall corrections applied to the Datasonde thermistor measurements are generally good below 60 km, it is possible that the correction term applied for lag is inadequate. Between 48 and 60 km the instrument is falling from a colder to a warmer atmosphere. As a result the instrument measurements are lagging the ambient temperatures until the stratopause is reached. Thus the colder Datasonde results. At altitudes below the stratopause (i.e., between 30 and 48 km) the atmospheric temperature lapse rate reverses, becoming colder with decreasing height; the Datasonde temperature measurement continues to lag the actual ambient temperature. Thus the warmer Datasonde result. The perturbations shown on the mean difference curve are believed to be coming from vertical motions affecting the sphere measurements and to a lesser extent from time and space differences between the two rocketsonde observations.

Recent measurements of the OH-radical rotational temperatures (D. Offermann, private communication, 1991) using a ground-based infrared (IR) spectrometer [*Baker et al.*, 1985] resulted in relatively excellent agreement with the falling sphere temperatures. Figure 7 illustrates one example of a falling sphere temperature profile obtained on the west coast of France during February 1990 and an independent measurement of the OH temperature retrieval. The ground-based IR spectrometer scanned periodically (once every 3 min) the intensities of the three rotational lines $P_1(2)$, $P_1(3)$, and $P_1(4)$ of the (3,1) band which lies close to 1.53 μm. The OH* temperature of Figure 7 based on the three scans was

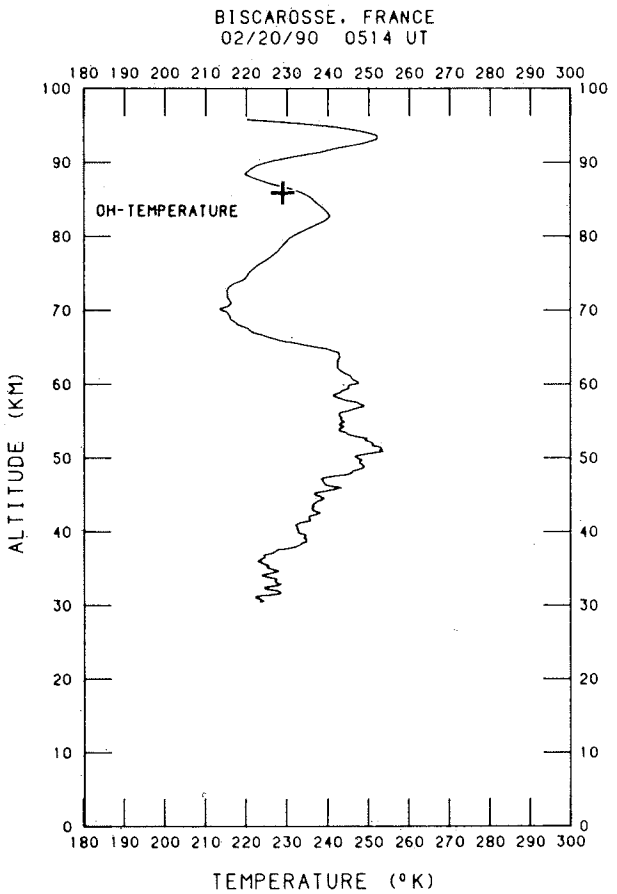

Fig. 7. Recent sphere temperature profile obtained during February 1990, near Bordeaux, France, showing good agreement with a remotely measured temperature of the OH* temperature prevalent near 86 km.

made between 0324 and 0333 UT. The mean temperature for this observation is 229°K. On the basis of the earlier work of *Baker et al.* [1985] and *von Zahn et al.* [1987] it can be assumed that the OH* layer is centered at an altitude of 86 ± 4 km. A direct comparison of the sphere and OH* temperatures at a point is misleading since the OH* is integrated about the layer. A better comparison was performed (H. Graef, private communication, 1991) by applying the OH* weighting function to the sphere temperatures over the same (approximate) altitude interval, computing the radiances, summing them, and deriving an equivalent OH* temperature. In Figure 7 the OH* equivalent sphere temperature is 227°K. Thus in this example a mean temperature difference of approximately 2°K was measured over the layer. During this campaign, 12 correlative sphere-OH* temperature comparisons were made near Bordeaux, France. The result of the comparison was a mean temperature difference of 0.92°K and a standard deviation of 7.6°K; only two of the 12 pairs exceeded a difference of 10°K. The correlation is excellent and reinforces our postulation that the inflatable sphere provides accurate temperatures.

7. Conclusions

Through theoretical derivation, computer simulations, and comparison of measurements we have shown that the inflatable falling sphere provides accurate temperature data in spite of bias that might occur in the measurement of density. Density biases are linearly transferred to the calculated pressure. Thus the effect of the bias is canceled since the method of deriving the temperature depends on a form of the gas equation which uses the ratio of the pressure and density.

The falling sphere technique is only affected by vertical winds and not by other external factors, such as aerodynamic heating, solar radiation, etc.; therefore the accuracy of sphere temperatures is intrinsically better than the accuracy obtainable with other in situ sensors, such as the bead thermistor used with the Datasonde. As demonstrated, using the radiosonde or the Datasonde measured density at some initializing altitude and then integrating upward, a correct density profile will be obtained. Shown also was an example of a new density profile that did not change significantly from the original profile; this is important because it indicates that a linear bias was not present in this particular measurement, i.e., the initial measurements were good. The examples discussed in section 5 also suggest that good sphere density data can be ensured by recalculating new densities through upward integration of all sphere measurements, when possible. Hence the procedure of recalculating sphere densities from an initial level of integration, if adopted, will strengthen the validity of the original density data.

Discrepancies between sphere and Datasonde densities and temperatures observed above 60 km lead to the conclusion that the corrections applied to the in situ thermistor measurements are not adequate at these levels. It must be recognized that the thermistor corrections above 60 km were originally derived from extrapolations. More work is necessary to improve the thermistor corrections, especially above 60 km, if the in situ thermistor measurement technique is to continue to be used in the future. Alternatively, given sufficient measurement pairs, a better estimate of the correction to be applied to Datasonde temperatures at the higher altitudes could possibly be determined using sphere temperatures as truth. Independent comparisons between falling spheres and remotely measured OH* temperatures near 86 km have also been shown to agree quite well. This illustrates that error introduced in the reduction due to the initial data point obtained from a model atmosphere is reduced considerably or disappears by the time the sphere reaches 85 km. The simulations and the analysis have shown that the inflatable sphere can provide accurate high altitude temperatures and would be well utilized to establish the accuracy of other high altitude temperature sensors. Because of the greater altitude coverage of the sphere system, more effective calibration and verification comparisons can be made with operational satellite data and with research satellite data such as will be available from UARS, EOS, and others. This is an important aspect, especially in relation to the "greenhouse" effect whereby significant stratospheric and mesospheric cooling is predicted [*Hansen et al.*, 1988]. Also, considering the inherent accuracy of the sphere temperatures, a better understanding of the vertical winds might be obtained from the perturbations seen in the sphere density and temperature data. Further simulations will include random variation of the vertical wind component which, hopefully, will enable a more precise interpretation of vertical wind motions to be made. Comparisons of the perturbations contained in the sphere temperature profile

against the more stable Datasonde temperature profile will also help in this effort.

In conclusion, the high accuracy of the sphere temperatures opens a completely new aspect of upper stratospheric, mesospheric, and lower thermospheric temperature measurement capability and application. The sphere temperature measurements could be a useful standard, primarily above 50 km altitude, that can be used to validate temperature measurements from other instruments and can be used to better understand the capabilities of the different measuring systems.

Acknowledgments. The authors wish to thank D. Offermann of the University of Wuppertal, Wuppertal, Germany, for the use of the sphere and OH* temperature data obtained during the recent DYANA Campaign. We also thank H. Graef, also of the University of Wuppertal, for making available the results of the differences between the integrated sphere-OH* temperatures.

REFERENCES

Angell, J. K., Rocketsonde evidence for a stratospheric temperature decrease in the western hemisphere during 1973–85, *Mon. Weather Rev.*, *115*, 2569–2577, 1987.

Baker, D. J., A. J. Steed, G. A. Ware, D. Offermann, G. Lange, and H. Lauche, Ground-based atmospheric infrared and visible emission measurements, *J. Atmos. Terr. Phys.*, *47*(1), 133–145, 1985.

Committee for the Extension of the U.S. Standard Atmosphere (COESA), (1976).

Engler, N. A., Development of methods to determine winds, density, pressure, and temperature from the ROBIN falling balloon, *AFCRL-65-448*, Univ. of Dayton Res. Inst., Dayton, Ohio, 1965.

Engler, N. A., and M. Dietenberger, Analysis of conjunctive rocketborne inflatable sphere and bead thermistor soundings, report to Atmospheric Sciences Laboratory, White Sands Missile Range, *Rep. ASL-CR-780013-1*, 24 pp., White Sands, N. M., 1978.

Engler, N. A., and J. K. Luers, Modifications to the 1972 robin program, final report to Atmospheric Sciences Laboratory, White Sands Missile Range, under contract DAEA18-77-C-0008, *Rep. ASL-CR-0008-1*, 45 pp., White Sands, N. M., 1978.

Finger, F. G., M. E. Gelman, F. J. Schmidlin, R. Leviton, and B. W. Kennedy, Comparability of meteorological rocketsonde data as indicated by international comparison tests, *J. Atmos. Sci.*, *32*, 1705–1714, 1975.

Hansen, J., I. Fung, A. Lacis, D. Rind, S. Lebedeff, R. Ruedy, and G. Russell, Global climate changes as forecast by Goddard Institute for Space Studies three-dimensional model, *J. Geophys. Res.*, *93*(D8), 9341–9364, 1988.

Horvath, J. J., and J. S. Theon, Response of the neutral particle upper atmosphere to the solar eclipse of 7 March 1970, *J. Atmos. Terr. Phys.*, *34*, 593–599, 1972.

Krumins, M. V., and W. C. Lyons, Corrections for the upper atmosphere temperatures using a thin film loop mount, *NOLTR 72-152*, 52 pp., Nav. Ord. Lab., Silver Spring, Md., 1972.

Leviton, R., and W. E. Palmquist, A rocket balloon instrument, *Bull. Am. Meteorol. Soc.*, *40*, 374, 1960.

Lübkin, F. J., and U. von Zahn, Simultaneous temperature measurements in the mesosphere and lower thermosphere during the MAC/EPSILON campaign, *Planet. Space Sci.*, *37*(10), 1303–1314, 1989.

Luers, J. K., A method of computing winds, density, temperature, pressure, and their associated errors from the high altitude ROBIN sphere using an optimum filter, contract F19628-C-0102, *AFCRL-70-0366*, Univ. of Dayton Res. Inst., Dayton, Ohio, 1970.

Olsen, R. O., and F. J. Schmidlin, Atmospheric thermal structure during a winter anomaly absorption event, *Space Res.*, *18*, 147–150, 1978.

Philbrick, C. R., A. C. Faire, D. H. Fryklund, Measurements of atmospheric density at Kwajalein Atoll, 18 May 1977, *Rep. AFGL TR 78-0058*, 113 pp., Air Force Geophys. Lab., 1978. (Available as *NTIS AD#054784* from Natl. Tech. Inf. Serv., Springfield, Va.)

Philbrick, C. R., F. J. Schmidlin, K. U. Grossmann, G. Lange, D. Offermann, K. D. Baker, D. Krankowsky, and U. von Zahn, Density and temperature structure over Northern Europe, *J. Atmos. Terr. Phys.*, *47*, 159–172, 1985.

Quiroz, R., and M. Gelman, An evaluation of temperature profiles from falling sphere soundings, *J. Geophys. Res.*, *81*(3), 406–412, 1976.

Schmidlin, F. J., Repeatability and measurement uncertainty of the United States meteorological rocketsonde, *J. Geophys. Res.*, *86*, 9599–9603, 1981.

Schmidlin, F. J., Intercomparisons of temperature, density, and wind measurement from in situ and satellite techniques, *Adv. Space Res.*, *4*(6), 101–110, 1984.

Schmidlin, F. J., Rocket techniques used to measure the middle atmosphere, in *Middle Atmosphere Program, Handbook for MAP*, vol. 19, edited by R. A. Goldberg, pp. 1–33, SCOSTEP Secretariat, Univ. of Ill., Urbana, 1986.

Schmidlin, F. J., E. T. Northam, and W. R. Michel, Results of wind simulations in the mesosphere using precision C-band radars and the inflatable falling sphere technique, paper presented at Conference on Aerospace and Range Meteorology, pp. 37–43, Am. Meteorol. Soc., Huntsville, Ala., August 27–29, 1985.

Schmidlin, F. J., H. S. Lee, and W. Michel, Improved resolution of atmospheric density measurements based on simulations, in 8th ESA Symposium on European Rocket and Balloon Programs and Related Research, Sunne, Sweden, May 17–23, 1987, *ESA SP-270*, pp. 133–138, Eur. Space Agency, Neuilly, France, 1987.

Smith, W. S., L. B. Katchen, and J. S. Theon, Grenade experiments in a program of synoptic meteorological measurements, in *Meteorological Monographs*, vol. 9, *Meteorological Investigations of the Upper Atmosphere*, edited by R. S. Quiroz, pp. 170–175, American Meteorological Society, Boston, Mass., 1968.

Theon, J. S., W. S. Smith, J. F. Casey, and B. R. Kirkwood, The mean observed meteorological structure, and circulation of the stratosphere and mesosphere, *NASA Tech. Rep. TR R-375*, 80 pp., 1972.

von Zahn, U., K. H. Fricke, R. Gerndt, and T. Blix, Mesospheric temperatures and the OH layer height as derived from ground-based lidar and OH* spectrometry, *J. Atmos. Terr. Phys.*, *49*, 863–869, 1987.

H. S. Lee, Science and Engineering Services, Inc., Silver Spring, MD 20904.

W. Michel, University of Dayton Research Institute, Wallops Island, VA 23337.

F. J. Schmidlin, NASA GSFC/Wallops Flight Facility, Wallops Island, VA 23337.

(Received September 21, 1990;
revised September 3, 1991;
accepted September 9, 1991.)